Dangling bonds in amorphous silicon investigated by Multifrequency EPR

M. Fehr[a], A. Schnegg[a], B. Rech[a], K. Lips[a], O. Astakhov[b], F. Finger[b], R. Bittl[c], C. Teutloff[c]

[a] *Helmholtz-Zentrum Berlin für Materialien und Energie, Institut für Silizium-Photovoltaik, Kekuléstr. 5, 12489 Berlin, Germany*
[b] *Forschungszentrum Jülich, Institut für Energie- und Klimaforschung, Photovoltaik, 52425 Jülich, Germany*
[c] *Freie Universität Berlin, Fachbereich Physik, Arnimallee 14, 14195 Berlin, Germany*

Abstract

Paramagnetic coordination defects in undoped hydrogenated amorphous silicon (a-Si:H) are studied using Multifrequency pulsed electron-paramagnetic resonance (EPR) spectroscopy at S-, X-, Q- and W-Band microwave frequencies (3.6, 9.7, 34, and 94 GHz, respectively). The improved spectral resolution at high magnetic field and the application of a multifrequency fitting procedure allows us to conclude that the g-tensor exhibits a rhombic splitting instead of axial symmetry. Our methods allow a highly precise and accurate determination of the g-tensor principal values $g_x = 2.0079(2)$, $g_y = 2.0061(2)$ and $g_z = 2.0034(2)$ and the distribution parameters (g-strain).

Keywords: electron paramagnetic resonance, defects, dangling bond, amorphous silicon, hydrogenated amorphous silicon, g value, hyperfine interaction

1. Introduction

Hydrogenated amorphous silicon (a-Si:H) is an important semiconductor material for thin-film solar cells and transistors. The performance of devices based on this material is mainly determined by paramagnetic defect states in the mobility gap acting as recombination centers for excess charge carriers. They exhibit a electron-paramagnetic resonance (EPR) spectrum with a g-value of $g = 2.0050 - 2.0055$ [1] whose intensity is routinely used as a measure for the electronic quality of a-Si:H [2]. In addition to defects present after material deposition, light illumination increases the defect density by about one order of magnitude [3]. This light-induced degradation phenomenon, known as the Staebler-Wronski effect (SWE) [4, 5], represents a significant limitation of the maximum efficiency of solar cells based on a-Si:H [6]. It is clear that a refined understanding of the defect generation process requires a resolution of the defect structure on the nano scale [6].

While there is a general consensus in the research community that deep defect centers in a-Si:H are intrinsic coordination defects, it is debated whether the defects arise due to over- (fivefold) or undercoordinated

Email address: matthias.fehr@helmholtz-berlin.de (M. Fehr)

(threefold) Si atoms, where the latter are usually denoted as dangling-bond (DB) defects. EPR is an ideal technique to resolve this controversy and to determine the local atomic structure of defects by measuring the g-tensor, i.e. the orientation dependent g-value, and hyperfine interactions (HFI) of the unpaired electron with nuclear spins of nearby H and Si atoms. After a experimental determination of these EPR parameters, the obtained values need to be compared to theoretical values of different defect structure models to concluded about the microscopic structure of defects. However, intrinsic defects in compounds with lightweight atoms such as Si often exhibit only a slight shift of the principal g-tensor values from the free-electron g-factor $g_e = 2.0023$. Hence, highly accurate and precise determination of these values is mandatory for a comparison with theory and a identification of the microscopic defect structure.

A detailed analysis of the EPR spectrum of coordination defects in a-Si:H was first carried out by Stutzmann *et al.* and Umeda *et al.* [1, 7]. They determined the g-tensor of the unpaired electron spin to be axially symmetric with principal values similar to the P_b center occurring at the Si/SiO_2 interface [8, 9] (see Table 1). However, in both studies the g-tensor was already assumed as axially symmetric in the fitting models and never systematically tested against rhombic symmetry.

Here, we present a detailed experimental investigation of the g-tensor symmetry and principal values of the dominant defect center in a-Si:H. The analysis of defects in a-Si:H is complicated by the fact that pronounced site-to-site variations of the principal g-values (g-strain) restrict the determination of principal A-values at high resonance frequencies. Since the determination of the principal g-values relies essentially on a complete simulation of the EPR spectrum, both quantities have to be determined. We therefore apply multifrequency EPR (S-band: 3.6 GHz/0.13 T, X-band: 9.7 GHz/0.34 T, Q-band: 34 GHz/1.2 T and W-band: 94 GHz/3.35 T), i.e. a combination of low-field and high-field EPR spectroscopy to separate field-independent ($\boldsymbol{A}$) and field-dependent ($\boldsymbol{g}$) spectral contributions.

2. Materials and Methods

Undoped a-Si:H samples were deposited with plasma-enhanced chemical vapor deposition (PECVD) on a 10 cm × 10 cm Mo foil from undiluted silane (silane concentration 100%) at the substrate temperature of about 185 °C (Further deposition parameters: pressure 0.7 mbar, power density 130 mW/cm^2, interelectrode distance 12 mm, deposition rate 1.8 nm/s). The initial defect density of the samples as determined by c.w. EPR is given by $N_D = 4(1) \cdot 10^{16}$ cm^{-3}. The hydrogen content of the sample is about 21 at. % as determined on a reference a-Si:H sample using Fourier-transform infrared spectroscopy. The films were removed from the substrate by diluted hydrochloric acid and flakes were collected in EPR-quartz tubes (see Ref. [10] for further information). Pulsed EPR spectroscopy at S-, X- and Q-band was performed on a Bruker BioSpin ElexSys E580 spectrometer and EPR measurements at W-band were performed on an ElexSys E680 spectrometer. The probe heads employed at S-, X- and W-Band were a Bruker ER4118S-MS5, a

Bruker ER4118X-MD5, and a Bruker EN600-1021H, respectively. At Q-band a home-built probe head was used. All experiments were carried out at a temperature of 80 K and utilized a field-swept echo (FSE) pulse sequence ($\pi/2 - \tau - \pi - \tau -$ echo) with a π pulse length of 40 ns, 32 ns, 80 ns, 128 ns and an interpulse delay τ of 400 ns, 300 ns, 400 ns, 300 ns at S-, X-, Q-, W-band, respectively. Spectra were independent of τ (data not shown) and the shot-repetition time was set sufficiently long to avoid a saturation of the spin system (> 2 ms). EPR spectra were accumulated about 1.5 h at Q- and W-band, and about 10 h at S- and X-band.

3. Results and Discussion

Fig. 1 depicts FSE spectra of a-Si:H powder samples taken at different microwave frequencies (S-, X-, Q- and W-band, respectively). In the left column (Fig. 1 a-d) experimental spectra taken at indicated frequency bands (crosses) are shown together with simulations obtained with parameters given in Table 1 (red solid lines).

The S- and X-band spectra (see Fig. 1 a,b) consist of an intense central line and two less intense satellite peaks (see enlarged spectral regions in Fig. 1a,b). The complex structure of the EPR spectrum originates from an isotope composition of naturally abundant Si, which is composed of stable non-magnetic isotopes ($^{28/30}$Si) with a total abundance of 95.32 %, and one stable magnetic isotope (^{29}Si) with an abundance of 4.68 % [11]. If the immediate vicinity of the defect is depleted from magnetic isotopes (^{29}Si and ^{1}H) large HFIs are absent, resulting in the narrow central line, which is broadened by unresolved HFI to more distant ^{1}H and ^{29}Si nuclei [7, 12]. In cases, however, where Si atoms, which exhibit a significant spin density, are magnetic (^{29}Si isotope), the EPR spectrum is dominated by large HFIs (> 150 MHz, equivalent to > 7 mT) giving rise to satellite formation in the EPR spectrum.

With increasing resonance frequency, the central line and the satellites exhibit increasing asymmetric line broadening, which may be attributed to g-anisotropy and g-strain. Therefore, the satellites, which are still resolved at X-band frequencies, overlap with the central line at Q- and W-band. Since the resolution of the principal g-values requires high frequencies, it becomes impossible to extract the magnetic parameters at one single frequency. It is therefore necessary to carry out a multifrequency study and to fit the EPR spectra in order to extract the g-tensor, $\boldsymbol{g}$, and the hyperfine tensor, $\boldsymbol{A}$. Both are 3x3 matrices with the principal values (g_x, g_y, g_z) and (A_x, A_y, A_z), respectively.

~~In~~ our fitting model includes magnetic-field dependent broadening induced by g-strain explicitly as an uncorrelated gaussian distribution of the principal values. As in earlier studies we treat only one ^{29}Si nuclear spin explicitly (hyperfine tensor denoted by $\boldsymbol{A}_{\mathrm{L}}$). The HFIs of all other spin carrying nuclei (such as ^{1}H, ^{29}Si) are assumed to be unresolved and are taken into account by a Voigtian line broadening function [1, 7]. As in the case of $\boldsymbol{g}$, the principal values of $\boldsymbol{A}_{\mathrm{L}}$ are distributed (A-strain) and we included this effect

in the simulation as an uncorrelated gaussian distribution of the principal values. Furthermore we make the following assumptions: i) the A_L-tensor is axially symmetric, ii) $\boldsymbol{A}_L$ and $\boldsymbol{g}$ are collinear with g_z and A_z being parallel and iii) the principal values of $\boldsymbol{A}_L$ are not correlated to the principal values of $\boldsymbol{g}$ (uncorrelated g- and A-strain).

To extract the A- and g-values we applied the following step-wise fitting routine. In a first step, the Q- and W-band spectra were fitted simultaneously by adjusting the distribution parameters of the three principal g-values (mean value and standard deviation). In a second step, the S- and X-band spectra were fitted by adjusting the distribution parameters of the A_L-tensor principal values, where we again assumed independent normal distributions. In a third step, the S-band spectrum was fitted by adjusting a convolutional Voigtian line broadening function accounting for inhomogeneous broadening by unresolved HFI. The three steps were repeated in a loop until convergence is reached. The simulations of the individual solid-state EPR spectra were performed with EasySpin, a MATLAB (The Mathworks, Natick, MA, USA) toolbox [13]. The simulated spectra are fitted to the experimental spectra by nonlinear least-squares methods using a trust-region-reflective algorithm implemented in MATLAB [14, 15].

In earlier publications [1, 7] it was explicitly assumed that the g-tensor is axially symmetric, i.e. $g_x = g_y = g_\perp$ and $g_z = g_\parallel$. In order to test this hypothesis, we performed two separate multifrequency fits. In a first fit the symmetry of the g-tensor is forced to axial symmetry and in a second fit no assumptions about the symmetry were made. In the first case the principal values of the g-tensor are $g_x = g_y = 2.0065(2)$ and $g_z = 2.0042(2)$ (fit shown by red solid line in Fig. 1 i-l), in very good agreement with earlier studies (see Ref. [7] and Table 1). In the second case we obtained a rhombic g-tensor with three different principal values ($g_x = 2.0079(2)$, $g_y = 2.0061(2)$ and $g_z = 2.0034(2)$) (fit shown by red solid line in Fig. 1 a-d). The goodness of the fit, as seen by comparing the fit to the experiment in Fig. 1 and measured quantitatively by the sum of squares of the fit residuals $\|r\|_2^2$ (difference between the fitted and the experimental spectra) is significantly worse in the case of an axially symmetric g-tensor as compared to a rhombic g-tensor (see Table 1). On the basis of our fit results and the corresponding statistical and systematic errors, we can state that g_x and g_y do not coincide on a significance level of $\approx 5\sigma$, hence we conclude that coordination defects in a-Si:H exhibit a rhombic g-tensor.

For the A_L-tensor we obtained $A_x = A_y = 151(13)$ MHz and $A_z = 269(21)$ MHz, which corresponds to $A_{iso} = 190(11)$ MHz and $A_{dip} = 39(8)$ MHz. These values are slightly smaller than the previously reported ones (see Table 1). The Voigtian broadening function, accounting for unresolved HFI, deviates only slightly from a pure Lorentzian function since the FWHM of the Gaussian component is about a factor of 4 smaller than the FWHM of the Lorentzian component (see Table 1). A complete overview of the various fit parameter sets including literature values is given in Table 1.

The multifrequency fitting results show that there is a peculiar symmetry deviation between the g-tensor and the hyperfine tensor $\boldsymbol{A}_L$. This can be explained in the following way. In the most simple case, the

unpaired electron of the paramagnetic dangling bond (undercoordinated Si atom) resides in a sp^x hybrid orbital. Since the hyperfine interaction is basically a ground-state property the A_L tensor is expected to exhibit the same axial symmetry as the sp^x hybrid orbital. The g-tensor, however, is a more complex quantity, for which we have to take into accout the complete electronic structure of the defect and not only the local ground-state spin-density distribution in the vicinity of specific nuclei. In the picture of second order perturbation theory [16], the most important contribution to the g-tensor arises from the interplay of the singly-occupied DB orbital with all other unoccupied or occupied orbitals weighted by their inverse energetic separation. An axially symmetric g-tensor requires degeneracy of a subset of the other orbitals, a condition which is not fullfilled in an amorphous solid like a-Si:H. The orbital degeneracy which can be present in the case of crystalline solids is broken by the intrinsic disorder and a g-tensor without axial symmetry properties arises.

4. Conclusion

In conclusion our multifrequency EPR approach to identify defects in amorphous silicon yields improved values for the g-tensor of the paramagnetic center. By testing the hypothesis of an axially-symmetric g-tensor we found that a more accurate model is a rhombic g-tensor with the following principal values: $g_x = 2.0079(2)$, $g_y = 2.0061(2)$ and $g_z = 2.0034(2)$. Due to the use of high-field EPR we could also increase the precision of the g-tensor principal values which is a highly desirable goal for a future comparison of the experimental values to theory. We furthermore discovered that there is a fundamental difference in the symmetry of the g-tensor (rhombic symmetry) and the hyperfine interaction tensor (axial symmetry), which can be attributed to the fact that the g-tensor reflects the complete electronic structure of the defect while the hyperfine tensor probes only the local spin-density distribution in the vicinity of the corresponding nuclei.

Acknowledgments

Financial support from BMBF (EPR-Solar network project 03SF0328) is acknowledged. C. Freysoldt and G. Pfanner (MPI Düsseldorf, Germany) together with M. Stutzmann and M. Brandt (TU Munich, Germany) are gratefully acknowledged for helpful discussions.

References

[1] M. Stutzmann, D. K. Biegelsen, Microscopic nature of coordination defects in amorphous silicon, Phys. Rev. B 40 (1989) 9834–9840.

[2] M. Stutzmann, The defect density in amorphous silicon, Philos. Mag. B 60 (1989) 531–546.

[3] H. Dersch, J. Stuke, J. Beichler, Light-induced dangling bonds in hydrogenated amorphous silicon, Appl. Phys. Lett. 38 (1981) 456–458.

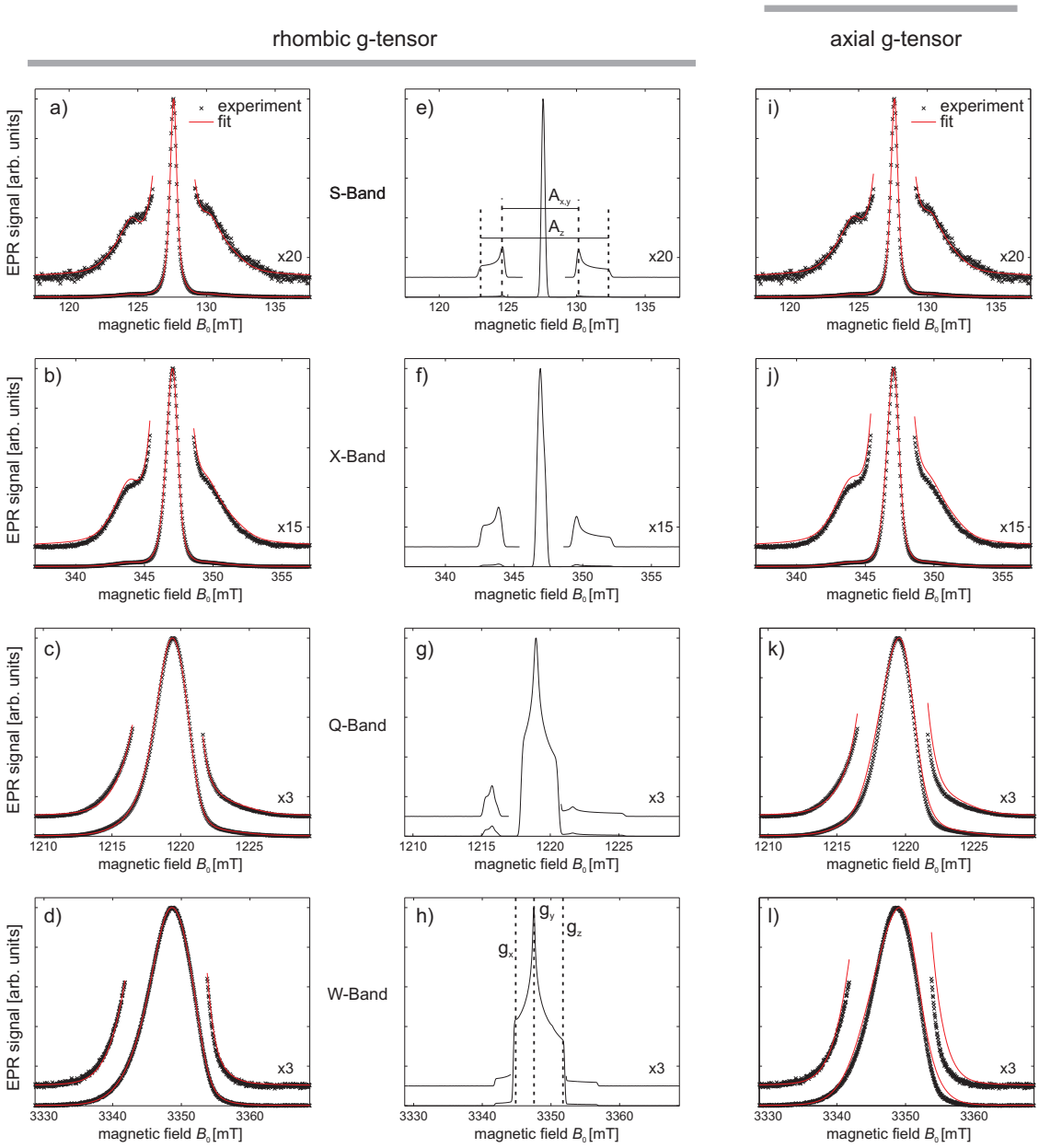

Figure 1: S-/X-/Q- and W-band field-swept echo EPR spectra of defects in a-Si:H ($g = 2.0055$) at a temperature of 80 K. Each spectrum was recorded by integrating the primary echo of a ($\pi/2 - \tau - \pi - \tau -$ echo) pulse sequence. Left column (a-d): experimental spectra (crosses) and the fitted spectra (red solid line) obtained with a g-tensor of rhombic symmetry. Spectra are offset vertically for clarity. middle column (e-h): fitted spectra for a rhombic g-tensor without g-strain, A-strain and isotropic magnetic field broadening. Principal values of the g-tensor and the A_L-tensor are indicated by the vertical and horizontal lines in e) and h). Right column (i-l): experimental spectra (crosses) and the fitted spectra (red solid line) obtained with an axially symmetric g-tensor.

Table 1: Summary of experimental (multifrequency fit) g-tensor and A_L-tensor principal values for coordination defects in a-Si:H. Full-width half maximum (FWHM) of gaussian distributions of the g- and A_L-tensor principal values (g- and A-strain) are given in square brackets. The Voigt function accounting for magnetic-field independent broadening is characterized by FWHM of Gaussian and Lorentzian components denoted by $\Delta B^{G/L}$. Standard errors of the fit parameters indicate a significance level of 1σ and are given in round brackets. $\|r\|_2^2$ denotes the sum of squares of the fit residual r in units of the sum of squares of the experimental data.

	principal values of g-tensor			principal values of ^{29}Si A_L-tensor				broadening function	
	g_x or $g_\perp$ [strain][1]	g_y or $g_\perp$ [strain][1]	g_z or $g_\parallel$ [strain][1]	A_x or $A_\perp$ [strain] in MHz^2	A_y or $A_\perp$ [strain] in MHz^2	A_z or $A_\parallel$ [strain] in MHz^2	A_{iso}/A_{dip} in MHz^2	Voigtian $\Delta B^{G/L}$ in mT	$\|r\|_2^2$ in %
(EPR)									
Present[3]	2.0079(2) [0.0054(1)]	2.0061(2) [0.0022(1)]	2.0034(2) [0.0018(1)]	151(13) [46(27)]	151(13) [46(27)]	269(21) [118(66)]	190(11)/39(8)	0.13(3)/0.43(1)	0.2
Present[4]	2.0065(2) [0.0047(1)]	2.0065(2) [0.0047(1)]	2.0042(2) [0.0019(1)]	149(15) [47(32)]	149(15) [47(32)]	265(26) [113(75)]	188(13)/39(10)	0.15(3)/0.42(1)	0.3
Ref. [7]	2.0065 [N/A][5]	2.0065 [N/A][5]	2.0039 [N/A][5]	143 [56]	143 [56]	333 [73]	206/63	N/A[5]	
Ref. [1]	2.0080 [0.0029]	2.0080 [0.0029]	2.0040 [0.0022]	154 [28]	154 [28]	305 [56]	205/50	not specified	

[4] D. L. Staebler, C. R. Wronski, Reversible conductivity changes in discharge-produced amorphous si, Appl. Phys. Lett. 31 (1977) 292–294.

[5] D. L. Staebler, C. R. Wronski, Optically induced conductivity changes in discharge-produced hydrogenated amorphous silicon, J. Appl. Phys. 51 (1980) 3262–3268.

[6] H. Fritzsche, Development in understanding and controlling the staebler-wronski effect in a-si:h, Annu. Rev. Mater. Res. 31 (2001) 47–79.

[7] T. Umeda, S. Yamasaki, J. Isoya, K. Tanaka, Electron-spin-resonance center of dangling bonds in undoped a-si:h, Phys. Rev. B 59 (1999) 4849–4857.

[8] E. H. Poindexter, P. J. Caplan, B. E. Deal, R. R. Razouk, Interface states and electron spin resonance centers in thermally oxidized (111) and (100) silicon wafers, J. Appl. Phys. 52 (1981) 879–884.

[9] M. Cook, C. T. White, Hyperfine interactions in cluster models of the p_b defect center, Phys. Rev. B 38 (1988) 9674–9685.

[10] L. H. Xiao, O. Astakhov, F. Finger, Silicon thin film powder samples for electron spin resonance investigation: Role of substrate and preparation procedure, Jpn. J. Appl. Phys. 50 (2011) 071301.

[11] D. K. Biegelsen, M. Stutzmann, Hyperfine studies of dangling bonds in amorphous silicon, Phys. Rev. B 33 (1986) 3006–3011.

[12] M. S. Brandt, M. W. Bayerl, M. Stutzmann, C. F. O. Graeff, Electrically detected magnetic resonance of a-si:h at low magnetic fields: the influence of hydrogen on the dangling bond resonance, J. Non-Cryst. Solids 227-230 (1998) 343–347.

[13] S. Stoll, A. Schweiger, Easyspin, a comprehensive software package for spectral simulation and analysis in epr, J. Magn. Res. 178 (2006) 42–55.

[14] T. F. Coleman, Y. Li, An interior trust region approach for nonlinear minimization subject to bounds, Siam J. Optim. 6

(1996) 418–445.

[15] T. F. Coleman, Y. Li, On the convergence of interior-reflective newton methods for nonlinear minimization subject to bounds, Math. Program. 67 (1994) 189–224.

[16] A. J. Stone, Gauge invariance of g tensor, Proc. R. Soc. London, Ser. A 271 (1963) 424–434.